



HAL
open science

Improved Adaptive High-Order Sliding Mode-Based Control for Trajectory Tracking of Autonomous Underwater Vehicles

Jesus Guerrero, Ahmed Chemori, Vincent Creuze, Jorge Torres

► **To cite this version:**

Jesus Guerrero, Ahmed Chemori, Vincent Creuze, Jorge Torres. Improved Adaptive High-Order Sliding Mode-Based Control for Trajectory Tracking of Autonomous Underwater Vehicles. IEEE Journal of Oceanic Engineering, inPress, pp.1-13. 10.1109/JOE.2024.3381391 . lirmm-04605914

HAL Id: lirmm-04605914

<https://hal-lirmm.ccsd.cnrs.fr/lirmm-04605914>

Submitted on 8 Jun 2024

HAL is a multi-disciplinary open access archive for the deposit and dissemination of scientific research documents, whether they are published or not. The documents may come from teaching and research institutions in France or abroad, or from public or private research centers.

L'archive ouverte pluridisciplinaire **HAL**, est destinée au dépôt et à la diffusion de documents scientifiques de niveau recherche, publiés ou non, émanant des établissements d'enseignement et de recherche français ou étrangers, des laboratoires publics ou privés.

Improved Adaptive High-Order Sliding Mode Based Control for Trajectory Tracking of Autonomous Underwater Vehicles

Jesus Guerrero^{*}, Ahmed Chemori[‡], Vincent Creuze[‡] and Jorge Torres[†]

^{*} Mechatronics Department, Tecnológico Nacional de México/ITS Abasolo, Mexico

[‡]LIRMM, Univ. Montpellier, CNRS, Montpellier, France

[†]Department of Automatic Control, CINVESTAV-IPN, CDMX, Mexico

Abstract—When an autonomous underwater vehicle is performing missions in the ocean it is often subject to external disturbances as the sea currents, changes in the salinity, etc. These phenomena could degrade the performance of the controller of the submarine which can be translated by increasing of the tracking error or causing instability. Taking into account these issues, in this paper we design an adaptive controller based on a high-order sliding mode control for an autonomous underwater vehicle focused on the paradigm of the trajectory tracking problem. First, we rewrite the classical representation of the underwater vehicle in terms of the known dynamics, and then it is transformed to a control affine structure. After, we design an adaptive high-order sliding mode controller for the trajectory tracking problem. Also, we prove the stability of the resulting closed-loop system using Lyapunov arguments. Finally, real-time experiments are performed to validate the proposed methodology as well as its robustness.

Index Terms—Sliding Mode Control, Underwater Vehicles, Adaptive Control, Trajectory Tracking.

I. INTRODUCTION

AUTONOMOUS underwater vehicles (AUVs) are versatile devices used in a large number of activities in the economic sector, security and surveillance, marine biology and archaeology, etc. For instance, they are used as platforms for monitoring of physical and chemical variables, surface mapping in marine geosciences, 3-D image reconstruction tasks and object recovery in marine archaeology, in marine pipelines monitoring, and so on. To gather an idea of its economical impact, let us emphasize that the autonomous underwater vehicle market is estimated to grow from USD 1.5 billion in 2021 to USD 4.3 billion by 2026, see [1].

The missions conducted by AUVs often require sophisticated control schemes to perform fine regulation tasks (station keeping) or trajectory tracking in adverse environments, due to sea currents, waves, or changes in external factors, such as pressure/depth, thermoclines of temperature, inherent to the marine environment. Therefore, there exists a real need for robust high-performance controllers for AUVs, which is a challenging task due to the complex nonlinear dynamics, with hydrodynamic parameters difficult to estimate and uncertain, in the presence of unpredictable external disturbances and

possibly changing environmental conditions [2]. For all these reasons, it is not surprising to notice that the control of AUVs has been the subject of continuous research since the 1990s. In the first stage, the control of AUVs was inspired by linear techniques, such as classical PID control [3], [4], linear optimal control [5], H_2 and H_∞ control [6], Model Predictive Control, etc. Undoubtedly, PID controllers and their different versions have been the most used with satisfactory results for certain operating conditions, [3], [7]–[10]; however, it is known that its performance may degrade when faced with of highly non-linear dynamics, uncertainties, time-varying parameters, [11], [12] etc.

In the search for robust control algorithms, one can mention, Fuzzy Logic Controllers (FLC) [13], Neural Networks (NNC) [14]; in general, these approaches lead to computational complex algorithms whose precision depends on the number of real-time trials, which may not be acceptable for its effective usage. Backstepping (BS) and Sliding Modes (SM) are robust nonlinear control techniques exhibiting excellent results for AUVs trajectory tracking control. Backstepping uses the kinematic model to generate virtual speed controls, while the dynamic model serves to design effective control laws to reach the virtual control references. Some particularities are the increase of derivatives of the desired trajectory with the dimension of the system, as well as eventual singularities in virtual control, [15], [13], [16], [17].

Sliding Modes Control is, by construction, robust against bounded external disturbances with finite-time convergence; however, the control signal chattering limited seriously its effective usage in real-time applications. One may counteract high-frequency control components by signum-like continuous functions, but at the cost of reducing robustness, since this constrains the sliding system's trajectories to the sliding surface's vicinity, [3], [18]. In turn, SMC with auto-adjustable gains or dynamical gains are a good alternative solution to somehow minimize the impact of the first-order SMC drawbacks, see [19], [20], respectively. High Order Sliding Mode Control (HOSMC) is a further development to reduce the chattering effect while preserving the robustness properties of the SMC. It is a quasi-continuous control driving both the sliding surface and its derivative to the origin, in the presence of smooth matched disturbances with a bound gradient [21].

This paper was produced by the IEEE Publication Technology Group. They are in Piscataway, NJ.

Manuscript received April 19, 2021; revised August 16, 2021.

The concept of adaptation seeks the systematic adjustment of gains, of controllers or observers, in order to preserve the nominal performance in presence of parametric variations or external disturbances. For instance, PID control may be enhanced by adaptive actions provided that hydrodynamic external forces and parametric uncertainties can be parameterized via a linear regressor in [22], [23]; in [24], a three-layer feedforward NN was used to identify unknown parameters along with adaptive laws to estimate the gains of the control algorithm. In [25], L1 adaptive control was proposed for depth and pitch trajectory control of an AUV. Adaptive trajectory tracking control under line-of-sight constraints has been transformed into a linear adaptive parametric problem [26].

The super-twisting algorithm (STA) is the simplest HOSMC algorithms and is recognized as the most powerful second-order SMC algorithm where the bound of the disturbance gradient must be known. This last may lead to unnecessarily large control gains due to the difficulties on estimating such a bound. To palliate this situation, an STA with adaptive gains preserving the convergence properties of both the sliding variables and its derivatives to the sliding manifold in the presence of a bounded disturbance of unknown bound was given in [20]. An adaptive second-order SMC for depth and yaw path following is proposed in [27]. A nonlinear function was introduced into the sliding surface to modify the damping ratio of the controller output. Then, the gain of the controller is estimated through the adaptive law which needs the disturbance's upper bound information. The efficiency of the proposed controller is demonstrated through real-time experiments. In [28], a multi-variable output feedback adaptive nonsingular terminal SMC for the four degrees of freedom trajectory tracking of AUV was developed. In this work, an adaptive observer with equivalent output injection was designed in order to estimate the system's states in finite time while the adaption control law stabilizes the trajectory tracking error to a small value in finite time. Through computer simulations, the effectiveness of the proposed controller was demonstrated compared to similar methodologies. Also, in [29], an adaptive second-order fast nonsingular terminal SMC for an AUV is proposed. In this work, the prior information about the upper bound of the disturbance is not required. Based on simulation results, chattering reduction and fast convergence is demonstrated when parameter uncertainties of 20 % and time variant disturbances were considered. In [30], an adaptive integral SMC for AUV stabilization was proposed. In this paper, two scenarios were considered. In the first case, it was assumed that the full system parameters were not available. In the second one, it was supposed that the system was affected by external disturbances. In both cases, the proposed adaptive law adjusted the feedback controller gains in order to suppress the chattering.

In this paper the interest is focused on adaptive high order sliding mode control for trajectory tracking of an AUV. The controller design is based on the Generalized Super Twisting Algorithm (GSTA) proposed in [31] which is basically composed of an standard STA together with an extra STA

linear correction term enhancing the convergence velocity and robustness of the algorithm. Recently, it was shown that GSTA with adaptation gains offers advantages from the theoretically and practical view point, namely; the knowledge on the bounds of the disturbance gradient is relaxed and over estimation of the controller gains with respect to the gain-fixed is reduced, [12]. Recently, Adaptive-gain GSTA was also proposed for trajectory tracking over an articulated intervention autonomous underwater vehicle (AIAUV), where it was exploited the fact that adaptive gains allows to handle both time-varying and state-dependant uncertainties which is crucial for AIAUVs. The results were validated in simulation and real-time experiments, so that the practical advantages of Adaptive GSTA over Adaptive STA or standard GSTA were nicely illustrated, [32].

However, according to the real-time experiments, the adaptive GSTA reported in [12], [32], the gain in the estimations remains increasing, which is the main problem of the original GSTA controller. To deal with this problem, a modification of the adaptive gains dynamics is proposed in this work. Basically, the suggested modification allows to change the sign of the change rate of both of the controller's gains. A complete stability analysis based on Lyapunov's stability theory is given. The performance and efficacy of the proposed strategy is evaluated in real-time experiments.

The rest of this paper is organized as follows. A concise description of the dynamic model of the underwater vehicle is given in Section II. The new adaptive proposed control technique is shown in Section III. In section IV, the real-time experimental results for trajectory tracking are presented and analyzed. Finally, some concluding remarks are outlined in Section V.

II. DYNAMIC MODEL OF UNDERWATER VEHICLES

The dynamic model of an underwater vehicle is defined through two reference frames (as illustrated in Fig. 1), the body-fixed frame and the earth-fixed frame. The dynamical model described in the body-fixed frame is given as follows:

$$M\dot{\nu} + C(\nu)\nu + D(\nu)\nu + g(\eta) = \tau + w_\nu(t) \quad (1)$$

where $\nu = [u, v, w, p, q, r]^T$ is the vector of velocity relative to the body-fixed frame. $M \in \mathbb{R}^{6 \times 6}$ is the inertia matrix, $C(\nu) \in \mathbb{R}^{6 \times 6}$ is the Coriolis-centripetal matrix, $D(\nu) \in \mathbb{R}^{6 \times 6}$ is the hydrodynamic damping matrix, $g(\cdot) \in \mathbb{R}^6$ is the vector which contains the gravitational and buoyancy forces and moments. $\tau \in \mathbb{R}^6$ is the control input vector acting on the vehicle and $w_\nu(t) \in \mathbb{R}^6$ is the vector of external disturbances. For a deeper description of the dynamic model, the reader can be referred to [3], [33].

The dynamics of the underwater vehicle can be transformed to the earth-fixed frame through the matrix of spatial transformation $J(\eta)$, as follows:

$$\dot{\eta} = J(\eta)\nu \quad (2)$$

where $\eta = [x, y, z, \phi, \theta, \psi]^T$ is the vector of position and orientation w.r.t. the earth-fixed frame and, $\dot{\eta}$ is the velocity

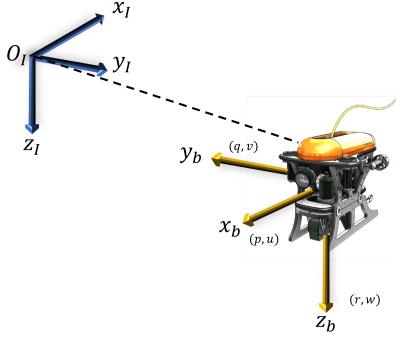


Fig. 1. Underwater vehicle with the body-fixed frame (O_b, x_b, y_b, z_b) and the world-fixed frame (O_I, x_I, y_I, z_I) .

vector. Then, replacing the transformation given by Eq. (2) in Eq. (1), leads to:

$$\underbrace{M_\eta(\eta)\dot{\eta} + C_\eta(\nu, \eta)\dot{\eta} + D_\eta(\nu, \eta)\dot{\eta} + g_\eta(\eta)}_{f(\nu, \eta)} = \tau_\eta(\eta) + \bar{w}_\eta(t) \quad (3)$$

where the matrices and vectors are defined as:

$$\begin{aligned} M_\eta(\eta) &= J^{-T}(\eta) M J^{-1}(\eta) \\ C_\eta(\nu, \eta) &= J^{-T}(\eta) \left[C(\nu) - M J^{-1}(\eta) \dot{J}(\eta) \right] J^{-1}(\eta) \\ D_\eta(\nu, \eta) &= J^{-T}(\eta) D(\nu) J^{-1}(\eta) \\ g_\eta(\eta) &= J^{-T}(\eta) g(\eta) \\ \tau_\eta(\eta) &= J^{-T}(\eta) \tau \\ \bar{w}_\eta(t) &= J^{-T}(\eta) w_\nu(t) \end{aligned}$$

From the model (3), we can observe that it depends on the hydrodynamic parameters of the vehicle. These parameters are difficult to estimate for all vehicle operating conditions as mentioned in [11]. For this reason, it is possible to rewrite the left part of the dynamics (3) in terms of the estimated $\hat{f}(\cdot)$, and unknown $\tilde{f}(\cdot)$ dynamics as follows:

$$f(\eta, \nu) = \hat{f}(\eta, \nu) + \tilde{f}(\eta, \nu) \quad (4)$$

where:

$$\hat{f}(\eta, \nu) = \hat{M}_\eta(\eta)\dot{\eta} + \hat{C}_\eta(\nu, \eta)\dot{\eta} + \hat{D}_\eta(\nu, \eta)\dot{\eta} + \hat{g}_\eta(\eta) \quad (5)$$

$$\tilde{f}(\eta, \nu) = \tilde{M}_\eta(\eta)\dot{\eta} + \tilde{C}_\eta(\nu, \eta)\dot{\eta} + \tilde{D}_\eta(\nu, \eta)\dot{\eta} + \tilde{g}_\eta(\eta) \quad (6)$$

Substituting (4) (6) into (3), yields the following dynamic model:

$$\hat{M}_\eta(\eta)\dot{\eta} + \hat{C}_\eta(\nu, \eta)\dot{\eta} + \hat{D}_\eta(\nu, \eta)\dot{\eta} + \hat{g}_\eta(\eta) = \tau_\eta(\eta) + w_\eta(t) \quad (7)$$

It is worth to note that the dynamics are rewritten in terms of the known hydrodynamic parameters $\hat{f}(\cdot)$ and the lumped vector $w_\eta(t)$ including the unknown dynamics and the bounded external disturbances as follows:

$$\omega_\eta(t) = \bar{w}_\eta - \tilde{f}(\cdot) \quad (8)$$

Note also that the dynamic model (7) can be rewritten in an affine control structure if we select the following state variables:

$$x_1 = \eta \quad ; \quad x_2 = \dot{\eta}$$

This state variable selection leads to the following nonlinear system:

$$\begin{aligned} \dot{x}_1 &= x_2 \\ \dot{x}_2 &= \hat{F}(x) + \hat{G}(x)u(t) + w(t) \end{aligned} \quad (9)$$

where:

$$\begin{aligned} \hat{F}(x) &= -\hat{M}_\eta(\eta)^{-1} \left[\hat{C}_\eta(\nu, \eta)\dot{\eta} + \hat{D}_\eta(\nu, \eta)\dot{\eta} + \hat{g}_\eta(\eta) \right] \\ \hat{G}(x) &= \hat{M}_\eta(\eta)^{-1} J^{-T}(\eta) \\ w(t) &= \hat{M}_\eta(\eta)^{-1} \bar{w}(t) \\ u(t) &= \tau_\eta \end{aligned}$$

Finally, some assumptions are required before introducing the design of the proposed adaptive controller:

Assumption 1. *The pitch angle remains smaller than $\pi/2$, i.e., $|\theta| < \pi/2$.*

Assumption 2. *The perturbation $w(t)$ is a Lipschitz continuous function.*

The assumption A1 ensures the existence of the inverse of the matrix $J(\eta)$ and as a consequence, the term $g(x)$ always exists. In a physical scenario, a pitch near to $\pi/2$ implies that the robot dives vertically, which is generally not required during sea missions.

The assumption A2 is a classical assumption in the paradigm of sliding mode control. However, in this work we only required to know the disturbance boundary but not necessarily to know the upper bound exactly. Based on this assumption, we can state the following condition:

$$|\dot{w}_i(t, x)| \leq L_i |\phi_2(\sigma)|, \quad i = \overline{1, \bar{6}} \quad (10)$$

with $L_i \geq 0$ is a finite unknown boundary.

III. ADAPTIVE HIGH-ORDER SLIDING MODE CONTROLLER DESIGN

In this section, the design of the proposed adaptive high order sliding mode control for the underwater vehicle is detailed. This controller is based on the Generalized Super Twisting Algorithm (GSTA) proposed in [31], which is a second order sliding mode control. This methodology ensures finite time convergence to the origin and is robust towards bounded external disturbances. The controller proposed in [34] have two feedback gains, which are tuned, in general, heuristically when it is applied through real-time experiments.

In [12], [16], we applied and extended the results of [34] to the case of MIMO systems, and based on the adaption methodology given in [35], we formulated an adaptive approach for the GSTA. However, based on the real-time experiments performed on an AUV, the gain in the estimations remains increasing as the main problem of the original controller. To deal with this problem, we improve the performance of the

proposed methodology by introducing a modification in the dynamics of the gain, which allows to change the sign of the change rate of both of the controller's gains.

The main result of our approach is summarized in the following theorem.

Theorem 1. *Given the underwater vehicle model dynamics by Eq. (7), suppose that the external disturbance term $w(t)$ is bounded and satisfies (10). Then for any initial conditions $x(0)$, $\sigma(0)$ the sliding surface $\sigma = 0$ will be reached in finite time via the following adaptive controller:*

$$\tau_\eta = J^T \hat{M}_\eta(\eta) [\ddot{x}_1^d(t) + \Lambda \dot{e}(t) - \hat{F}(x) - v] \quad (11)$$

where $\Lambda = \text{diag}(\lambda_1, \lambda_2, \dots, \lambda_6) > 0$ is a diagonal matrix with constant gains, $\ddot{x}_1^d(t)$ is the second-time derivative of the desired trajectory, v is the Adaptive Generalized Super-Twisting Algorithm expressed as follows:

$$\begin{aligned} v &= -K_1(t)\Phi_1(\sigma) + \lambda \\ \dot{\lambda} &= -K_2(t)\Phi_2(\sigma) \end{aligned} \quad (12)$$

with the vectors $\Phi_1 = [\phi_{1,1}, \phi_{1,2}, \dots, \phi_{1,6}]^T$ and $\Phi_2 = [\phi_{2,1}, \phi_{2,2}, \dots, \phi_{2,6}]^T$, where each element of those vectors is defined as follows:

$$\begin{aligned} \phi_{1,i} &= \mu_{1,i} |\sigma_i|^{\frac{1}{2}} \text{sgn}(\sigma_i) + \mu_{2,i} \sigma_i \\ \phi_{2,i} &= \frac{1}{2} \mu_{1,i}^2 \text{sgn}(\sigma_i) + \frac{3}{2} \mu_{1,i} \mu_{2,i} |\sigma_i|^{\frac{1}{2}} \text{sgn}(\sigma_i) + \mu_{2,i}^2 \sigma_i \end{aligned}$$

with $\mu_{1,i}, \mu_{2,i} \geq 0$ for $i = \overline{1,6}$. The controller feedback gains are defined as $K_1(t) = \text{diag}(k_{1,1}(t), k_{1,2}(t), \dots, k_{1,6}(t))$ and $K_2(t) = \text{diag}(k_{2,1}(t), k_{2,2}(t), \dots, k_{2,6}(t))$ such that $K_1(t) = K_1(t)^T > 0$ and $K_2(t) = K_2(t)^T > 0$. Furthermore, each element of the matrices K_1 and K_2 is defined through the following adaption law:

$$\dot{k}_{1i}(t) = \begin{cases} \omega_i \sqrt{\frac{\varsigma_i}{2}} \text{sgn}(|\sigma_i| - \mu_i) & \text{if } k_{1i} > k_{min}^i \\ \bar{\eta}_i & \text{otherwise} \end{cases} \quad (13)$$

$$k_{2i}(t) = 2\epsilon_i k_{1i}(t) + \beta_i + 4\epsilon_i^2 \quad (14)$$

where $\omega_i, \varsigma_i, \beta_i, \mu_i, k_{min}^i, \bar{\eta}_i$, and ϵ_i are arbitrary positive constants for $i = \overline{1,6}$. Then, for any initial condition $\sigma_i(0)$, the sliding surface $\sigma_i = 0$ will be reached in finite time.

Proof. Consider the following sliding surface:

$$\sigma(t) = \dot{e}(t) + \Lambda e(t) \quad (15)$$

where $\sigma(t) := [\sigma_1, \sigma_2, \dots, \sigma_6]^T$, $e(t) = x_1^d(t) - x_1(t)$ is the error vector, $x_1(t)$ is the state vector, and $x_1^d(t)$ is the desired trajectory defined as:

$$x_1^d(t) = [x_d(t), y_d(t), z_d(t), \phi_d(t), \theta_d(t), \psi_d(t)]^T \quad (16)$$

Note that the time derivative of the error vector is expressed as:

$$\dot{e}(t) = \dot{x}_1^d(t) - \dot{x}_2 \quad (17)$$

Now, taking the time derivative of the sliding surface (15), leads to:

$$\dot{\sigma}(t) = \ddot{e}(t) + \Lambda \cdot \dot{e}(t) \quad (18)$$

where $\ddot{e}(t) = \ddot{x}_1^d - \ddot{x}_2$.

Injecting the control law (11) into (18), leads to:

$$\dot{\sigma} = -K_1(t)\Phi_1(\sigma) - K_2(t) \int_0^t \Phi_2(\sigma(\tau)) d\tau + w(t) \quad (19)$$

Now, consider the following change of variables:

$$\begin{aligned} z_{1i} &= \sigma_i \\ z_{2i} &= -k_{2i} \int_0^t \phi_{2i}(\sigma_i(\tau)) d\tau + w_i(t) \end{aligned}$$

Then, Eq. (19) can be rewritten in a scalar form ($i = \overline{1,6}$) as follows:

$$\begin{aligned} \dot{z}_{1i} &= -k_{1i} \left[\mu_{1i} |z_{1i}|^{\frac{1}{2}} \text{sgn}(z_{1i}) + \mu_{2i} z_{1i} \right] + z_{2i} \\ \dot{z}_{2i} &= -k_{2i} \left[\frac{1}{2} \mu_{1i}^2 \text{sgn}(z_{1i}) + \frac{3}{2} \mu_{1i} \mu_{2i} |z_{1i}|^{\frac{1}{2}} \text{sgn}(z_{1i}) + \mu_{2i}^2 z_{1i} \right] \\ &\quad + \frac{d}{dt} w_i(t, x) \end{aligned}$$

The system above can be rewritten using a simplified notation as follows:

$$\begin{aligned} \dot{z}_1 &= -k_1 \left[\mu_1 |z_1|^{\frac{1}{2}} \text{sgn}(z_1) + \mu_2 z_1 \right] + z_2 \\ \dot{z}_2 &= -k_2 \left[\frac{1}{2} \mu_1^2 \text{sgn}(z_1) + \frac{3}{2} \mu_1 \mu_2 |z_1|^{\frac{1}{2}} \text{sgn}(z_1) + \mu_2^2 z_1 \right] \\ &\quad + \frac{d}{dt} w(t, \chi) \end{aligned} \quad (20)$$

Then, the Lyapunov Function candidate is defined as:

$$V(z_1, z_2, k_1, k_2) = V_0(\cdot) + \frac{1}{2\varsigma_1} (k_1 - k_1^*)^2 + \frac{1}{2\varsigma_2} (k_2 - k_2^*)^2 \quad (21)$$

where $\varsigma_1, \varsigma_2, k_1^*, k_2^*$ are positive constants and $V_0(\cdot)$ is given by:

$$V_0(z_1, z_2, k_1, k_2) = \xi^T P \xi \quad (22)$$

with:

$$\xi^T = [\phi_1(z_1), z_2] \quad (23)$$

and

$$P = P^T = \begin{bmatrix} \beta + 4\epsilon^2 & -2\epsilon \\ -2\epsilon & 1 \end{bmatrix} > 0 \quad (24)$$

Since β and ϵ are defined as arbitrary positive constants, then P is a positive definite matrix. Moreover, note that the function $V_0(\cdot)$ satisfies the following:

$$\lambda_{min}(P) \|\xi\|_2^2 \leq V_0(z, k) \leq \lambda_{max}(P) \|\xi\|_2^2 \quad (25)$$

where $\lambda_{min}(P)$ and $\lambda_{max}(P)$ are the minimum and maximum eigenvalues of P , respectively. $\|\xi\|_2^2 = |z_1| + 2|z_1|^{\frac{3}{2}} + z_1^2 + z_2^2$ is the Euclidean norm of ξ and satisfying the following inequality:

$$|\phi(z_1)| \leq \|\xi\|_2 \leq \frac{V^{\frac{1}{2}}(\xi)}{\lambda_{min}^{\frac{1}{2}}(P)} \quad (26)$$

Finally, it is worth to emphasize that the proposed Lyapunov function candidate $V(\cdot)$ is a continuous, positive definite and differentiable function.

The procedure to find the time derivative of the function $V(\cdot)$ is divided into two main steps. First, the time derivative

of $V_0(\cdot)$ is found. Second, the total time derivative of $V(\cdot)$ is computed.

Step 1. Knowing that $\phi_2(z_1) = \phi_1'(z_1)\phi_1(z_1)$, the derivative of $V_0(\cdot)$ is obtained as follows:

$$\dot{V}_0 = 2\xi^T P \dot{\xi} \quad (27)$$

$$= 2\xi^T P \begin{bmatrix} \phi_1' \left[-k_1 \phi_1(z_1) + z_2 \right] \\ -k_2 \phi_2(z_1) + \frac{d}{dt} w(t, x) \end{bmatrix} \quad (28)$$

$$= 2\xi^T P \begin{bmatrix} \phi_1'(z_1) \left[-k_1 \phi_1(z_1) + z_2 \right] \\ \phi_1'(z_1) \phi_1(z_1) \left[-k_2 + L \right] \end{bmatrix} \quad (29)$$

$$= \phi_1'(z_1) 2\xi^T P \underbrace{\begin{bmatrix} -k_1 & z_2 \\ -(k_2 - L) & 0 \end{bmatrix}}_{A(t, x)} \xi \quad (30)$$

$$= \phi_1'(z_1) \xi^T (A^T(t, x) P + P A(t, x)) \xi \quad (31)$$

$$= -\phi_1'(z_1) \xi^T Q(t, x) \xi \quad (32)$$

where

$$Q(x, t) = \begin{bmatrix} 2k_1(\beta + 4\epsilon^2) - 4\epsilon(k_2 - L) & \star \\ k_2 - L - 2\epsilon k_1 - \beta - 4\epsilon^2 & 2\epsilon \end{bmatrix} \quad (33)$$

and $\star = k_2 - L - 2\epsilon k_1 - \beta - 4\epsilon^2$.

By selecting the gain $k_2 = 2\epsilon k_1 + \beta + 4\epsilon^2$, we have the following:

$$Q - 2\epsilon I = \begin{bmatrix} 2k_1\beta - 4\epsilon(\beta + 4\epsilon^2 - L) - 2\epsilon & -L \\ -L & 2\epsilon \end{bmatrix} \quad (34)$$

The matrix Q is positive definite with a minimal eigenvalue $\lambda_{\min}(Q) \geq 2\epsilon$ if

$$k_1 > \delta_0 + \frac{\alpha_2^2}{4\epsilon\beta} + \frac{\epsilon \left[2(\beta + 4\epsilon^2 + L) + 1 \right]}{2\beta} \quad (35)$$

Then, the time derivative of $V_0(\cdot)$ can be rewritten as:

$$\dot{V}_0 = -\phi_1'(z_1) \xi^T Q(t, x) \xi \leq -2\epsilon \phi_1'(z_1) \xi^T \xi \quad (36)$$

$$\dot{V}_0 = -2\epsilon \left(\mu_1 \frac{1}{2|z_1|^{\frac{1}{2}}} + \mu_2 \right) \xi^T \xi \quad (37)$$

Finally, using (26), the time derivative of $V_0(\cdot)$ is expressed as:

$$\dot{V}_0 \leq -\frac{\epsilon \lambda_{\min}^{\frac{1}{2}}(P)}{\lambda_{\max}(P)} \mu_1 V_0^{\frac{1}{2}}(z, k) - \frac{2\epsilon}{\lambda_{\max}(P)} \mu_2 V(z, k) \quad (38)$$

$$\leq -\gamma V_0^{\frac{1}{2}}(z, k) \quad (39)$$

with $\gamma = \mu_1 \frac{\epsilon \lambda_{\min}^{\frac{1}{2}}(P)}{\lambda_{\max}(P)}$.

Step 2. The time derivative of the Lyapunov function (21) is given by:

$$\begin{aligned} \dot{V} &= \dot{V}_0(\cdot) + \frac{1}{\varsigma_1} (k_1 - k_1^*) \dot{k}_1 + \frac{1}{\varsigma_2} (k_2 - k_2^*) \dot{k}_2 \\ &\leq -\gamma V_0^{\frac{1}{2}}(z, k) + \frac{1}{\varsigma_1} (k_1 - k_1^*) \dot{k}_1 + \frac{1}{\varsigma_2} (k_2 - k_2^*) \dot{k}_2 \\ &= -\gamma V_0^{\frac{1}{2}}(z, k) - \frac{\omega_1}{\sqrt{2\varsigma_1}} |k_1 - k_1^*| - \frac{\omega_2}{\sqrt{2\varsigma_2}} |k_2 - k_2^*| \\ &\quad + \frac{1}{\varsigma_1} (k_1 - k_1^*) \dot{k}_1 + \\ &\quad + \frac{1}{\varsigma_2} (k_2 - k_2^*) \dot{k}_2 + \frac{\omega_1}{\sqrt{2\varsigma_1}} |k_1 - k_1^*| + \frac{\omega_2}{\sqrt{2\varsigma_2}} |k_2 - k_2^*| \end{aligned}$$

Using the Cauchy-Schwarz inequality, the first three terms of \dot{V} can be synthesized as follows:

$$-\gamma V_0^{\frac{1}{2}}(z, k) - \frac{\omega_1}{\sqrt{2\varsigma_1}} |k_1 - k_1^*| - \frac{\omega_2}{\sqrt{2\varsigma_2}} |k_2 - k_2^*| \leq -\pi \sqrt{V(\cdot)} \quad (40)$$

where $\pi = \min(\gamma, \omega_1, \omega_2)$.

Assuming that there exist two positive constants k_1^* and k_2^* such that $k_1 - k_1^* < 0$ and $k_2 - k_2^* < 0$, $\forall t \geq 0$. Then, the time derivative of V can be rewritten as:

$$\begin{aligned} \dot{V} &\leq -\pi \sqrt{V(z, k_1, k_2)} - |k_1 - k_1^*| \left(\frac{1}{\varsigma_1} \dot{k}_1 - \frac{\omega_1}{\sqrt{2\varsigma_1}} \right) \\ &\quad - |k_2 - k_2^*| \left(\frac{1}{\varsigma_2} \dot{k}_2 - \frac{\omega_2}{\sqrt{2\varsigma_2}} \right) \\ &= -\pi \sqrt{V(z, k_1, k_2)} + \vartheta \end{aligned} \quad (41)$$

where:

$$\vartheta = -|k_1 - k_1^*| \left(\frac{1}{\varsigma_1} \dot{k}_1 - \frac{\omega_1}{\sqrt{2\varsigma_1}} \right) - |k_2 - k_2^*| \left(\frac{1}{\varsigma_2} \dot{k}_2 - \frac{\omega_2}{\sqrt{2\varsigma_2}} \right) \quad (42)$$

In order to preserve the finite-time convergence it is necessary to satisfy the condition $\vartheta = 0$, which can be achieved through the following adaption laws:

$$\dot{k}_1 = \omega_1 \sqrt{\frac{\varsigma_1}{2}} \quad (43)$$

$$\dot{k}_2 = \omega_2 \sqrt{\frac{\varsigma_2}{2}} \quad (44)$$

In brief, the adaptive gains k_1 and k_2 will be increased based on the dynamic and algebraic equations stated in (13) until the condition (35) is reached. Then, the matrix Q will be positive definite and the finite-time convergence will be assured according to (41). Finally, when the sliding variable σ and its derivative converge to zero, the adaptive gains k_1 and k_2 will stop growing by making $\dot{k}_1 = 0$ as $\sigma = 0$. Subsequently, the gain-adaptation law (13) is obtained. \square

IV. REAL-TIME EXPERIMENTAL RESULTS

In this section, the performance and the robustness towards external disturbances of the proposed control scheme is demonstrated through real-time experiments.

The experimental platform is called *Leonard*, and it was developed by the Laboratory of Computer Science, Robotics, and Microelectronics (LIRMM) of the University of Montpellier in France. This robot has six independent propellers to obtain a fully actuated propulsion system. The dimensions of *Leonard* are $750 \times 550 \times 450mm$ with a total weight of 28 kg.

The robot is equipped with some sensors on board in order to obtain the orientation and the depth of the vehicle. The data provided by the robot is sent to the control PC on the surface (CPU Intel Core i7-3520M 2.9 GHz, 8GB RAM). Then, the machine computes the control actions, and sends back the input signal to the actuators of the underwater vehicle. The technical information about the electronic system of the robot is summarized on Table I.

The real-time experiments were performed in a $4 \times 4 \times 1.2 \text{ m}^2$ pool at LIRMM laboratory. The controller proposed by Eq. (11) was designed for the 6 DoF of the robot. However, the experiments are focused on two among them, namely the depth and yaw dynamics. In all the conducted experiments, we propose a continuous desired trajectory depending on time, and the robot is controlled to track the given reference in spite of the external disturbances and parametric uncertainties.

A. Scenarios for Real-Time Experiments

The main objective of the proposed controller lies in the capability of the robot to track a given reference trajectory in yaw and depth simultaneously. In order to show the robustness of the proposed adaptive controller we conducted the following scenarios:

- *Trajectory tracking case:* In this scenario, the robot tracks a given reference trajectory under conditions, without external disturbances.
- *Trajectory tracking under parametric uncertainties:* In this experiment, the hydrodynamic parameters of the robot are modified. We have attached a plastic sheet and a pair of floats to the robot in order to modify both the damping and buoyancy of the vehicle.
- *Trajectory tracking under external disturbances:* In this test, the robot is aggressively pushed by a person using a stick in order to apply an external disturbance.

B. Performance Evaluation Criteria

To fairly compare the behavior of controllers, let us consider the following robustness evaluation criteria:

- The root mean square of the tracking error (RMSE), defined as follows:

$$\text{RMSE} = \left(\frac{1}{N} \sum_{i=1}^N (e_q[i])^2 \right)^{\frac{1}{2}} \quad (45)$$

where N represents the total number of samples, and e denotes the tracking error of the proper state q (depth or yaw).

- Integral Square Error (ISE) is defined as:

$$\text{ISE} = \int e_q^2 dt \quad (46)$$

- The Integral Absolute Error (IAE), expressed by:

$$\text{IAE} = \int |e_q| dt \quad (47)$$

where e_q is the tracking error signal in both cases, i.e. the ISE and the IAE.

- To evaluate the energy consumption of the proposed control algorithm, we consider the following input torque-based criterion:

$$\text{INT} = \sum_{i=1}^N |\tau_q[i]| \quad (48)$$

where $\tau_q = \tau_\eta$ is the control input.

TABLE I
ROOT MEAN SQUARE FOR THE IAGSTA CONTROLLER AND THE AGSTA,
FOR THE THREE PROPOSED SCHEMES

Scenario	RMSE (IAGSTA)		RMSE (AGSTA)	
	Depth	Yaw	Depth	Yaw
1	0.0005	0.3629	0.0013	0.2077
2	0.0013	0.6969	0.0196	0.1758
3	0.0011	0.5529	N.C.	N.C.

TABLE II
INTEGRAL SQUARE ERROR FOR THE IAGSTA CONTROLLER AND THE
AGSTA, FOR THE THREE PROPOSED SCHEMES

Scenario	ISE (IAGSTA)		ISE (AGSTA)	
	Depth	Yaw	Depth	Yaw
1	0.0897	9801	0.07	8158
2	0.1718	17157	22.19	29286
3	0.0011	0.5529	N.C.	N.C.

C. Trajectory tracking under Nominal conditions

The obtained experimental results for the nominal case are depicted in Fig. 2. At the top of the Figure, we can observe the evolution of both controllers for the depth and yaw tracking references (black dashed line). As we can see, the proposed controller (red line) has a better performance than the AGSTA (blue line). Indeed, the convergence to the reference signal of the proposed algorithm is better in both experiments. This behavior is clearly explained by the error plots shown at the middle of the Figure. Finally, the forces and torques generated by the controllers are depicted at the bottom of the Fig. 2. One can observe that chattering appears in the case of yaw tracking dynamics when the AGSTA is applied.

To demonstrate the superior performance of the proposed controller compared with the AGSTA, we computed several performance evaluation indicators. The RMSE values are summarized in Table I. The RMSE shows that the IAGSTA has a better performance than the AGSTA for the tracking on depth. However the AGSTA shows slightly better tracking than the IAGSTA for the yaw dynamics. The ISE indicator given in Table II shows a better behavior from the AGSTA compared to the proposed controller. Then, in Table III is shown the IAE indicator and we can observe that the AGSTA shows a better performance than the IAGSTA. Finally, in terms of energy consumption, the IAGSTA has a better performance than the AGSTA, this means that the proposed algorithm needs less energy and this is confirmed by analyzing the lower part of Fig. 2, this reduction in the energy consumption is due to the adaption of the gains.

In the Figure 3, the evolution versus time of the adaptive gains for the depth dynamics is shown. As we can see, the values of the gains are changing at the beginning of the experiments but converge to a constant steady-state value later.

In Fig. 4, we can observe the adaption of the gains of the yaw dynamics for the proposed controller. As we can see, the gain converges fast to a vicinity of a constant value, and remains there in the absent of external disturbances.

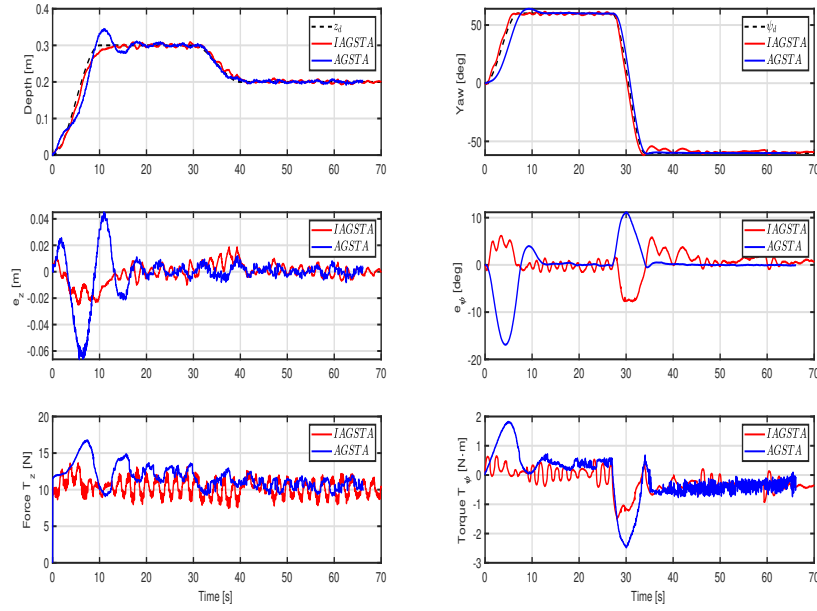


Fig. 2. Trajectory tracking of depth and yaw simultaneously. Comparison of the proposed adaptive controller versus the AGSTA. Top, trajectory tracking of depth (left) and yaw (right) dynamics. Middle, error plots of the proposed controller versus the AGSTA. Bottom, the evolution of the controller's input.

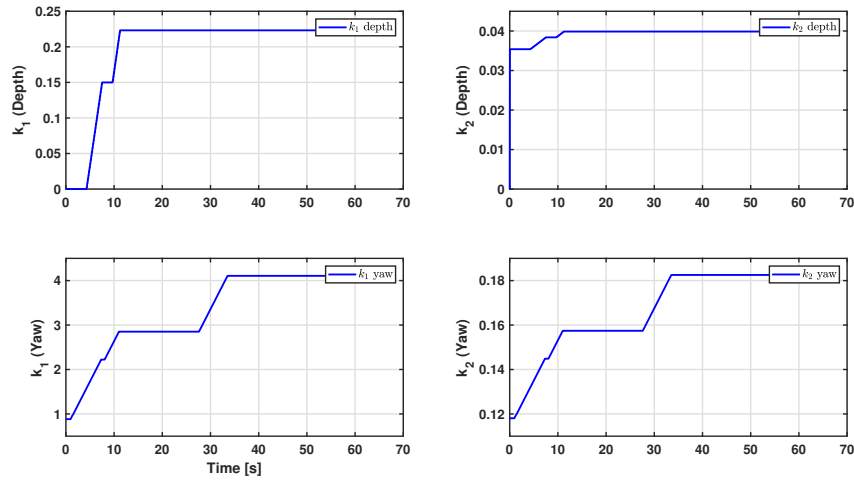


Fig. 3. Evolution versus time of the adaptive gains of the AGSTA controller.

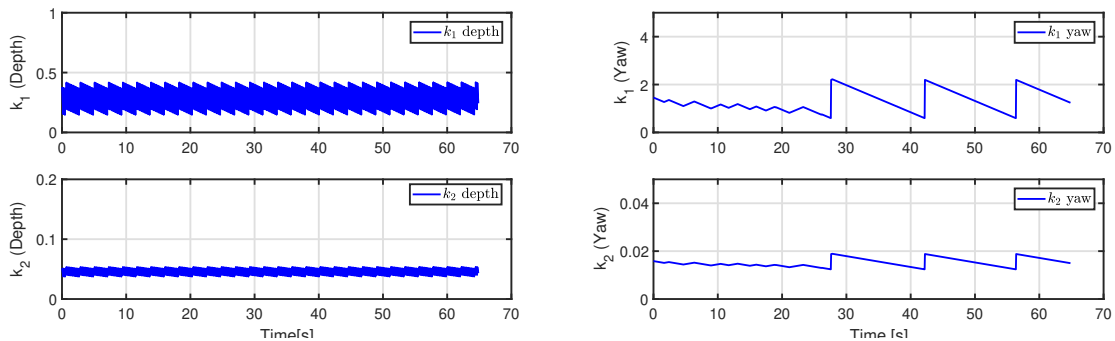


Fig. 4. Evolution versus time of the adaptive gains for the proposed controller IAGSTA.

TABLE III
INTEGRAL ABSOLUTE ERROR FOR THE IAGSTA CONTROLLER AND THE AGSTA, FOR THE THREE PROPOSED SCHEMES

Scenario	IAE (IAGSTA)		IAE (AGSTA)	
	Depth	Yaw	Depth	Yaw
1	9.82	2907	7.16	1569
2	15.26	4317	142.19	2896.3
3	0.0011	0.5529	N.C.	N.C.

TABLE IV
INPUT TORQUE BASED CRITERION FOR THE IAGSTA CONTROLLER AND THE AGSTA, FOR THE THREE PROPOSED SCHEMES

Scenario	INT (IAGSTA)		INT (AGSTA)	
	Depth	Yaw	Depth	Yaw
1	2824	417	17295	1005
2	6628	709	33349	1211
3	0.0011	0.5529	N.C.	N.C.

D. Trajectory tracking under parametric uncertainties case

Figure 6 shows the obtained results of the real-time experiments for the trajectory tracking when parametric uncertainties are considered. On one hand, to introduce uncertainties in the parameters for the depth dynamics, we attached two floats to the robot’s body in order to change its floatability. In theory, by adding these floaters we change the value of the vector $g(\eta)$ of the model (1), which is directly related to the depth dynamics. In the other hand, to modify the parameters of the yaw dynamics of the robot, we attached a rigid plastic sheet at one side of the vehicle as shown in Fig. 5. When the vehicle turns about the z-axis, the parameters of the vehicle change. In particular, the terms of the damping matrix ($D(\eta, \dot{\eta})$) will change.

Figure 6, shows the obtained results for the trajectory tracking test of this scenario. At the top of the Figure, we can observe the performance of the proposed controller and

the AGSTA. From this figure, we can note that the proposed controller converges faster than the AGSTA; however, this controller converges to a vicinity of the reference. While the AGSTA, converge to the reference in 15 seconds but it has a better behavior than the IAGSTA in steady-state regime. At the middle of Fig. 6, the plot of the tracking errors is shown, where we can see that the tracking error of the proposed algorithm is smaller than the one of AGSTA; however in steady state, the AGSTA has a smoother behavior. Finally, at the bottom of Fig. 6, the evolution versus time of the control input signal is plotted, the proposed controller needs a less energy consumption than the AGSTA; however the chattering effect appears in both cases.

The plot of the yaw trajectory tracking is shown on the upper-left part of Fig. 6. At the top of this figure 6, the performance of both controllers is plotted, we can observe that the proposed methodology has a better behavior than the AGSTA. The IAGSTA converges faster than the AGTSA; however, at time of 35 seconds, we can see that the AGSTA shows a better tracking performance than the proposed algorithm. At the middle of Fig. 6, one can see the tracking error plots, where the adaptive version shows a smaller tracking error than the AGSTA. At the bottom of Fig. 6, we can observe that the proposed controller shows a smoother evolution than the AGSTA. In fact, the AGSTA shows chattering from 35 seconds to the end of the experiment.

In Fig.7 we can observe the evolution versus time of the gains adaptation of the AGSTA. One can notice that the controller overestimates the gain and continuously increases its value, which can generate chattering in the vehicle’s thrusters, as we can see in the lower part of Fig. 6, where the chattering is visible in the torque of the yaw dynamics.

The evolution of the adaptive gains of the proposed controller is shown in the right part of Fig. 8. As in the previous case, the feedback gains take some time for auto tuning, due to the reference variation. However, as time increases, the gain converge to a constant value. As comparison, it is possible to observe that the evolution of the gain is similar to the nominal case.

In the left part of Fig. 8, we can observe the gain dynamics for the yaw tracking trajectory. As in the case of depth, the controller takes some time for the auto tuning task and after some seconds, it converges to a steady-state value. Again, the behavior of the dynamics is similar to the nominal case.

As a controller performance parameter, in Table I, the RMSE for this experiment is shown. In numerical terms, the proposed controller has a better behavior than the AGSTA for the depth dynamics. However, for the yaw tracking, the AGSTA shows a better performance than the IAGSTA. The ISE criterion is summarized in Table II, we can observe that the IAGSTA shows a better performance than the AGSTA. From the data summarized in Table III, we can conclude that the IAGSTA shows a better depth trajectory tracing than the AGSTA in terms of the IAE criterion. However, for the case of the yaw dynamics, the AGSTA has a lower numeric value than the IAGSTA. Finally, in terms of energy consumption, it is clear that the proposed IAGSTA has a lower level consumption when is compared with the AGSTA. This is also visible on

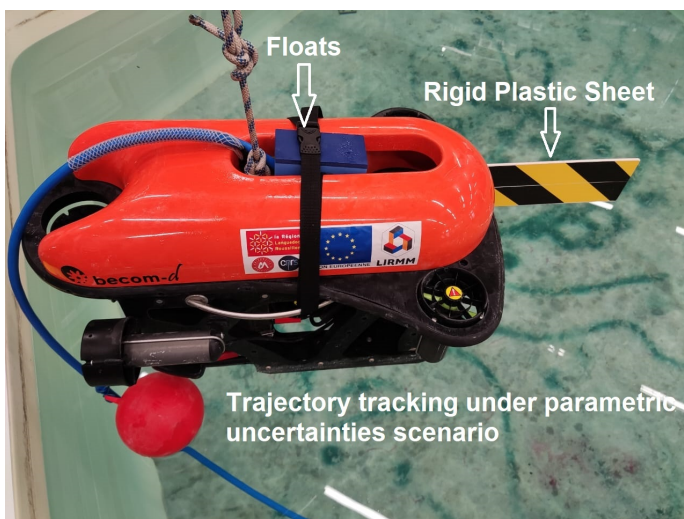


Fig. 5. Leonard robot with a rigid plastic sheet for the robustness toward parametric uncertainties case.

the lower part of Fig. 6.

E. Trajectory tracking under external disturbances case

In this scenario, we have applied a high impact external disturbances to the robot's body. When the vehicle tracks the references in depth and yaw, it was pushed with a broomstick in order to generate an external disturbance. In this scenario, we did not make a comparison with the AGSTA because it is not possible to reproduce exactly the same disturbance for both controllers in two different experiments.

At the top of Fig. 9, one can observe the performance of the IAGSTA under several external disturbances. As expected, the depth dynamics shows a good performance towards these aggressive disturbances. The yaw dynamics, tracks the reference without a significant change with respect the nominal case. At the middle of Fig. 9, the tracking errors for this scenario are plotted. Finally, at the bottom of Fig. 9, we can observe the evolution of the forces and torques generated by the thrusters. The curves shown in this graph are reasonable and do not represent a risk of damage for the actuators.

The adaption of the gains of the proposed controller is shown in Fig. 10. It is possible to observe the evolution of the gains when an external force is applied to the submarine. We can see that the adaption is very reactive and the gain can increase or decrease its value depending of the intensity of the disturbance.

In Tables I to IV, the performances criteria for this case are summarized.

V. CONCLUSION

In this paper we developed an adaptive controller based on a second order sliding mode control for the trajectory tracking problem of an Autonomous Underwater Vehicle.

First, we described the dynamic model in terms of the body-fixed frame, then this dynamics were transformed to the earth-fixed frame. After considering parametric uncertainties and external disturbances, we rewrote the dynamical model in terms of the known nominal parameters of the model.

Second, employing a proper selection of state variables, we can transform the vehicle's dynamics into an affine controller form. This structure simplifies the design of the adaptive sliding mode controller. Then, using a sliding surface based on the tracking error, we designed an adaptive controller based on SOSMC. The structure of the dynamic gain of the proposed controller prevent the overestimation of the adaptive gain. Compared with the AGSTA, this gain could increase or decrease depending on the magnitude of the tracking error.

Third, using Lyapunov arguments we proved the stability of the proposed controller.

Finally, we proposed three different experimental scenarios to test the robustness of the proposed algorithm. The control objective is to track a time varying reference in depth and yaw simultaneously in spite of parametric uncertainties and external disturbances. In particular, for the nominal case, where disturbances are not considered, the proposed controller has a faster convergence than the AGSTA. In the second

scenario, when we introduce uncertainties in the hydrodynamic parameters of the vehicle, also the proposed algorithm converge faster than the AGSTA and the energy consumption is lower than the previous adaptive version. In the last case, i.e. the trajectory tracking under external disturbances, the proposed controller shows a good performance in terms of recovery each disturbance.

ACKNOWLEDGMENTS

The *Leonard* underwater vehicle has been financed by the European Union (FEDER grant n° 49793) and the Region Occitanie (ARPE Pilot Plus project).

REFERENCES

- [1] U. Am-Mass, *Market Research Report: Autonomous Underwater Vehicle (AUV) Market*, ser. J. Mark. Res. A Marketing Ass. American Marketing Association (USA), 2021. [Online]. Available: ISSN-1547-7193
- [2] S. Zhao and J. Yuh, "Experimental study on advanced underwater robot control," *IEEE transactions on robotics*, vol. 21, no. 4, pp. 695–703, 2005.
- [3] T. I. Fossen, "Guidance and control of ocean vehicles," *University of Trondheim, Norway, Printed by John Wiley & Sons, Chichester, England, ISBN: 0 471 94113 1, Doctors Thesis*, 1999.
- [4] T. T. J. Prestero, "Verification of a six-degree of freedom simulation model for the remus autonomous underwater vehicle," Ph.D. dissertation, Massachusetts institute of technology, 2001.
- [5] da Silva Tchilian R., S. Rafikova E. and Gafurov, and R. M., "Optimal control of an underwater glider vehicle," *Procedia Eng.*, vol. 176, p. 732–740, 2017.
- [6] L. Moreira and C. Soares, "Sh2 and h designs for diving and course control of an autonomous underwater vehicle in presence of waves," *IEEE J. Ocean.*, vol. 33, no. 2, pp. 69–88, 2008.
- [7] P. Herman, "Decoupled pd set-point controller for underwater vehicles," *Ocean Engineering*, vol. 36, no. 6-7, pp. 529–534, 2009.
- [8] M. H. Khodayari and S. Balochian, "Modeling and control of autonomous underwater vehicle (auv) in heading and depth attitude via self-adaptive fuzzy pid controller," *Journal of Marine Science and Technology*, vol. 20, no. 3, pp. 559–578, 2015.
- [9] P. Sarhadi, A. R. Noei, and A. Khosravi, "Model reference adaptive pid control with anti-windup compensator for an autonomous underwater vehicle," *Robotics and Autonomous Systems*, vol. 83, pp. 87–93, 2016.
- [10] J. Guerrero, J. Torres, V. Creuze, A. Chemori, and E. Campos, "Saturation based nonlinear pid control for underwater vehicles: Design, stability analysis and experiments," *Mechatronics*, vol. 61, pp. 96–105, 2019.
- [11] E. Campos, A. Chemori, V. Creuze, J. Torres, and R. Lozano, "Saturation based nonlinear depth and yaw control of underwater vehicles with stability analysis and real-time experiments," *Mechatronics*, vol. 45, pp. 49–59, 2017.
- [12] J. Guerrero, J. Torres, V. Creuze, and A. Chemori, "Trajectory tracking for autonomous underwater vehicle: An adaptive approach," *Ocean Engineering*, vol. 172, pp. 511–522, 2019.
- [13] X. Xiang, L. Lapierre, C. Liu, and B. Jouvencel, "Path tracking: combined path following and trajectory tracking for autonomous underwater vehicles," in *2011 IEEE/RSJ International Conference on Intelligent Robots and Systems*. IEEE, 2011, pp. 3558–3563.
- [14] R. Cui, C. Yang, Y. Li, and S. Sharma, "Adaptive neural network control of auvs with control input nonlinearities using reinforcement learning," *IEEE Transactions on Systems, Man, and Cybernetics: Systems*, vol. 47, no. 6, pp. 1019–1029, 2017.
- [15] A. Aguiar and P. Joao, "Trajectory-tracking and path-following of underactuated autonomous vehicles with parametric modeling uncertainty," *IEEE Trans. Autom. Control*, vol. 52, no. 8, pp. 1362–1379, 2007.
- [16] J. Guerrero, J. Torres, E. Antonio, and E. Campos, "Autonomous underwater vehicle robust path tracking: Generalized super-twisting algorithm and block backstepping controllers," *Journal of Control Engineering and Applied Informatics*, vol. 20, no. 2, pp. 51–63, 2018.
- [17] A. S. Tijjani, A. Chemori, and V. Creuze, "Robust adaptive tracking control of underwater vehicles: design, stability analysis, and experiments," *IEEE/ASME Transactions on Mechatronics*, vol. 26, no. 2, pp. 897–907, 2020.

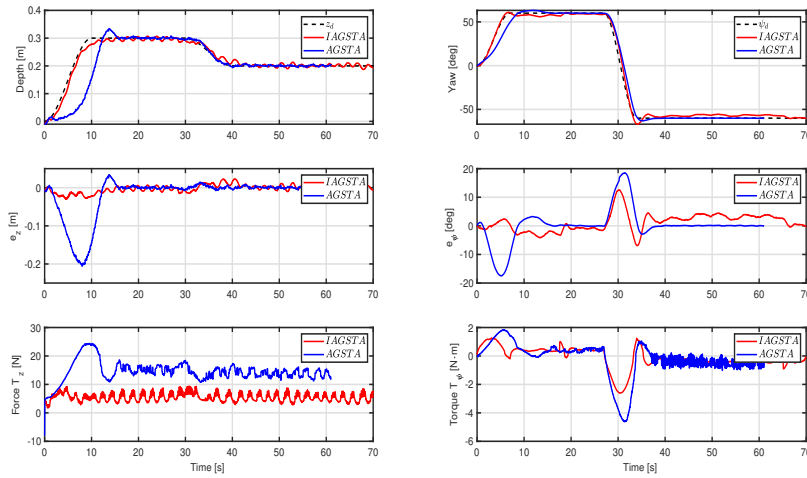


Fig. 6. Performance of the proposed controller under parameter uncertainties. (Top) Trajectory tracking in depth and yaw when the damping matrix and the gravity vector were modified. (Middle) Plots of the tracking error signal. (Bottom) Evolution of the control inputs.

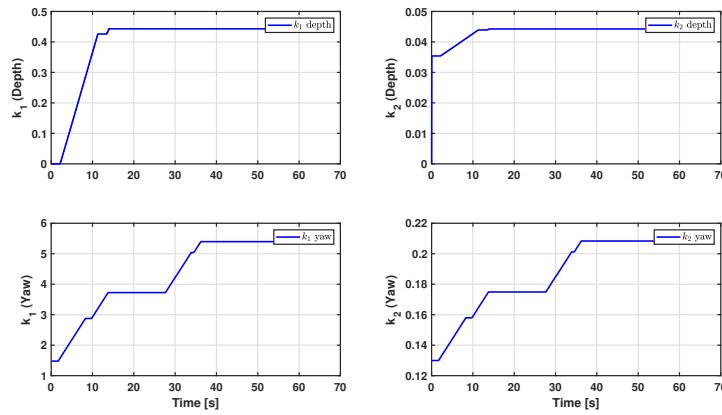


Fig. 7. Evolution versus time of the adaptive gains for the AGSTA controller.

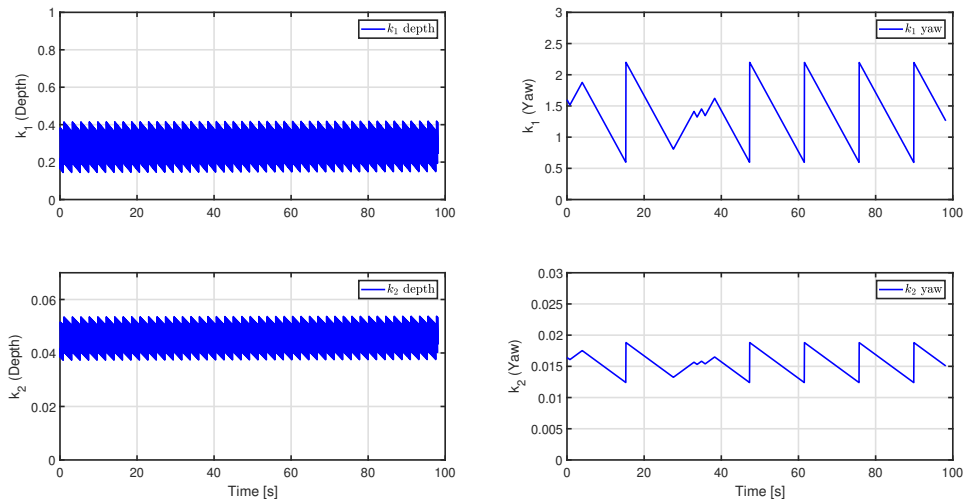


Fig. 8. Evolution versus time of the adaptive gains for the proposed controller IAGSTA.

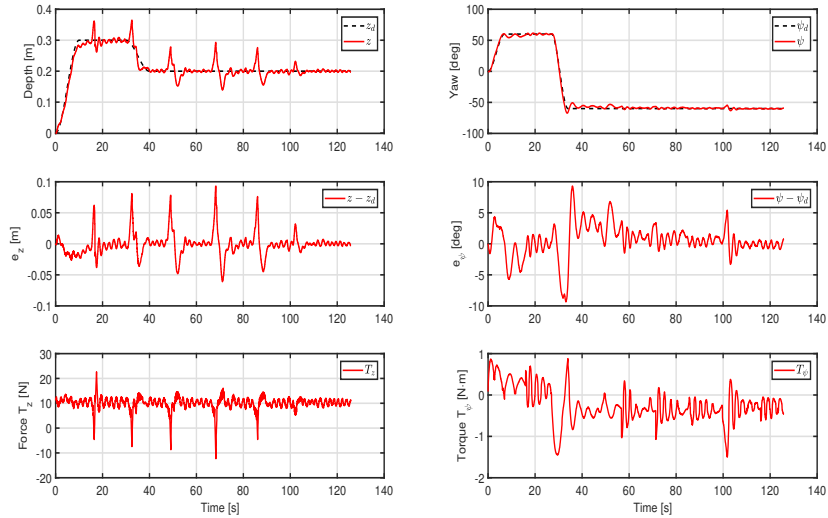


Fig. 9. Performance of the IAGSTA controller when is exposed to an aggressive external disturbances. (Top) Trajectory tracking of depth and yaw dynamics. (Middle) Plots of the error signal. (Bottom) Evolution of the control inputs.

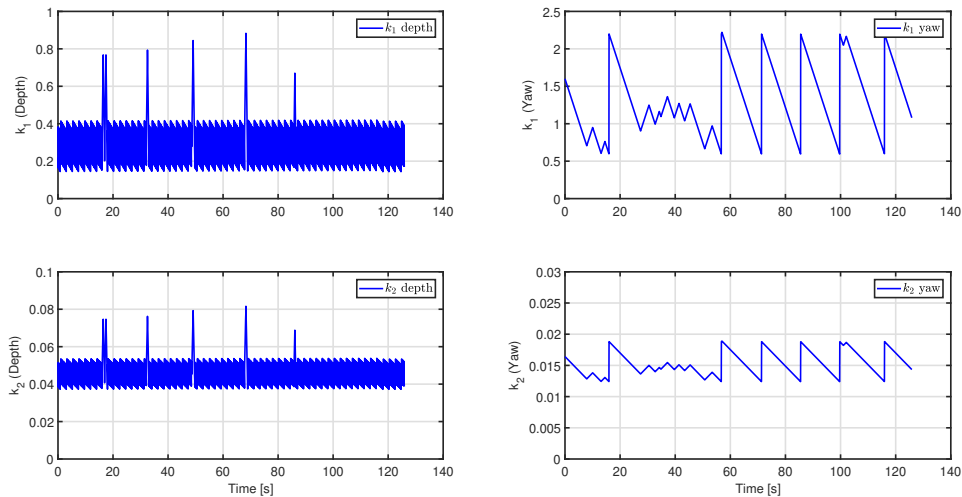


Fig. 10. Evolution of the adaptive gains for the proposed controller.

[18] Y. Shtessel, C. Edwards, L. Fridman, and A. Levant, *Sliding mode control and observation*. Springer, 2014, vol. 10.

[19] T. Gonzalez, J. A. Moreno, and L. Fridman, "Variable gain super-twisting sliding mode control," *IEEE Transactions on Automatic Control*, vol. 57, no. 8, pp. 2100–2105, 2012.

[20] Y. Shtessel, M. Taleb, and F. Plestan, "A novel adaptive-gain supertwisting sliding mode controller: Methodology and application," *Automatica*, vol. 48, no. 5, pp. 759–769, 2012.

[21] M. J. Castillo I, Fridman LM, "Super-twisting algorithm in presence of time and state dependent perturbations," *Int J Control*, vol. 91, no. 11, pp. 2535–2548, 2018.

[22] A. G., F. Caccavale, S. Chiaverini, and G. Fusco, "A novel adaptive control law for underwater vehicles," *IEEE Transactions on Control Systems and Technology*, vol. 11, no. 2, pp. 221–232, 2003.

[23] B. K. Sahu and B. Subudhi, "Adaptive tracking control of an autonomous underwater vehicle," *Int. Jour. Autom and Compt.*, vol. 11, no. 3, pp. 299–307, 2014.

[24] Z. Chu, D. Zhu, S. X. Yang, and G. E. Jan, "Adaptive sliding mode control for depth trajectory tracking of remotely operated vehicle with thruster nonlinearity," *The Journal of Navigation*, vol. 70, no. 1, pp. 149–164, 2017.

[25] D. Maalouf, A. Chemori, and V. Creuze, "L1 adaptive depth and pitch control of an underwater vehicle with real-time experiments," *Ocean Eng.*, vol. 98, pp. 66–77, 2015.

[26] J. Li, J. Du, G. Zhu1, and F. L. Lewis, "Simple adaptive trajectory tracking control of underactuated autonomous underwater vehicles under los range and angle constraints," *IET Control*, vol. 14, no. 2, pp. 283–290, 2022.

[27] G.-c. Zhang, H. Huang, L. Wan, Y.-m. Li, J. Cao, Y.-m. Su *et al.*, "A novel adaptive second order sliding mode path following control for a portable auv," *Ocean Engineering*, vol. 151, pp. 82–92, 2018.

[28] Y. Wang, L. Gu, M. Gao, and K. Zhu, "Multivariable output feedback adaptive terminal sliding mode control for underwater vehicles," *Asian Journal of Control*, vol. 18, no. 1, pp. 247–265, 2016.

[29] L. Qiao and W. Zhang, "Adaptive second-order fast nonsingular terminal sliding mode tracking control for fully actuated autonomous underwater vehicles," *IEEE Journal of Oceanic Engineering*, no. 99, pp. 1–23, 2018. [Online]. Available: <http://dx.doi.org/10.1109/JOE.2018.2809018>

[30] M. Sarfraz, F. u. Rehman, and I. Shah, "Robust stabilizing control of nonholonomic systems with uncertainties via adaptive integral sliding

mode: An underwater vehicle example,” *International Journal of Advanced Robotic Systems*, vol. 14, no. 5, p. 1729881417732693, 2017.

- [31] J. A. Moreno, “Lyapunov approach for analysis and design of second order sliding mode algorithms,” in *Sliding Modes after the first decade of the 21st Century*. Springer, 2011, pp. 113–149.
- [32] I.-L. Borlaug, K. Pettersen, and J. Gravdahl, “The generalized super-twisting algorithm with adaptive gains,” *Int J Robust Nonlinear Control*, vol. 32, no. 13, p. 7240–7270, 2022.
- [33] T. I. Fossen, *Marine control systems: guidance, navigation and control of ships, rigs and underwater vehicles*, 2002.
- [34] J. A. Moreno, “A linear framework for the robust stability analysis of a generalized super-twisting algorithm,” in *Electrical Engineering, Computing Science and Automatic Control, CCE, 2009 6th International Conference on*. IEEE, 2009, pp. 1–6.
- [35] F. Plestan, Y. Shtessel, V. Bregeault, and A. Poznyak, “New methodologies for adaptive sliding mode control,” *International journal of control*, vol. 83, no. 9, pp. 1907–1919, 2010.



Jesus Guerrero received his Ph.D. degree in 2019 in automatic control from the Center for Research and Advanced Studies of the National Polytechnic Institute (CINVESTAV), Mexico. He is currently a professor at the Department of Mechatronics of the Instituto Tecnológico Superior de Abasco. His research interests include nonlinear, adaptive and time-delay control and their applications in underactuated systems, ground, aerial, underwater vehicles, and bipedal robots.



Ahmed Chemori received his M.Sc. and Ph.D. degrees respectively in 2001 and 2005, both in automatic control from the Grenoble Institute of Technology. Then, he has been a Post-doctoral fellow for one year with the Automatic control laboratory of Grenoble. He is currently a tenured research scientist in Automatic control and Robotics at the Montpellier Laboratory of Informatics, Robotics, and Microelectronics. His research interests include nonlinear, adaptive and predictive control and their applications in humanoid robotics, underactuated systems, parallel robots,

and underwater vehicles.



Vincent Creuze received his Ph.D. degree in 2002 in robotics from the University Montpellier 2, France. He is currently an associate professor at the University Montpellier 2, attached to the Robotics Department of the LIRMM (Montpellier Laboratory of Computer Science, Robotics, and Microelectronics). His research interests include design, modelling, and control of underwater robots, as well as underwater computer vision.



Jorge Torres was born in Mexico City, on May 13, 1960. He received the B.S. degree in Electronic Engineering from the National Polytechnic Institute (IPN) of Mexico in 1982, the M.S. degree in Electrical Engineering from CINVESTAV-IPN, Mexico in 1985, and the Ph.D. degree in Automatic Control from LAG, INPG, France, in 1990. He joined the Department of Electrical Engineering at the CINVESTAV, Mexico, in 1990. He spent a sabbatical year, from September 1997 to August 1998, at the Institute of Research in Communications

and Cybernetics, IRCCYN-Nantes, France. Then, he served as the head of the Department of Automatic Control since its creation in September 1999 until January 2003, when he was called to serve as Secretary of Planning as a member of the Direction team of CINVESTAV, until March 2004. He was leading, from the Mexican side, the French Mexican Laboratory on Applied Automation (LAFMAA) of CNRS from January 2002 to January 2006. He was nominated as Deputy Director of the UMI 3175 LAFMIA at CINVESTAV Mexico, which is a joint research laboratory founded by CNRS, CINVESTAV and CONACYT for the period 2008–2012. His research interest lies in the structural approach of linear systems, stability of multivariate polynomials, and control of bioprocess for waste water treatment and control of mini-submarines